

# LHD Bootstrap Current Coefficient Calculations with the VENUS+ $\delta f$ code

Maxim Yu. ISAEV, Kiyomasa Y. WATANABE<sup>1</sup>, Masayuki YOKOYAMA<sup>1</sup>, Nobuyoshi OHYABU<sup>1</sup>,  
Craig D. BEIDLER<sup>2</sup>, Henning MAASSBERG<sup>2</sup>, Wilfred A. COOPER<sup>3</sup>, Trach-Minh TRAN<sup>3</sup>  
and Mikhail I. MIKHAILOV

*Russian Research Center “Kurchatov Institute”, Moscow, 123182, Russia*

<sup>1</sup>*National Institute for Fusion Science, Toki, 509-5292, Japan*

<sup>2</sup>*Max-Planck Institute für Plasma Physik, D-17491, Greifswald, Germany*

<sup>3</sup>*Centre de Recherches en Physique des Plasmas, CH-1015, Lausanne, Suisse*

(Received 18 November 2007 / Accepted 16 April 2008)

Normalized bootstrap current coefficients are calculated for Large Helical Device (LHD, Japan) plasma configurations with different magnetic axis positions using the VENUS+ $\delta f$  code [Fusion Sci. Technol. **50**, 440 (2006)]. The dependences on the different collisionality regimes (over the full experimental range of LHD plasma discharges) and the plasma radii are presented. The comparison of the VENUS+ $\delta f$ , SPBSC and DKES codes results is shown. The approach to the LHD experimental results is discussed. The bootstrap current effect on the  $iota = 1$  islands is considered.

© 2008 The Japan Society of Plasma Science and Nuclear Fusion Research

Keywords: heliotron, stellarator, magnetic configuration, neoclassical transport, bootstrap current, 3D numerical orbit,  $\delta f$  method

DOI: 10.1585/pfr.3.036

## 1. Introduction

The LHD is a superconducting large helical device with a helical field with poloidal winding number  $l = 2$  and  $m = 10$  toroidal field periods [1]. The LHD super dense core (SDC) plasma with a density  $4.5 \times 10^{20} \text{ m}^{-3}$ , the internal diffusion barrier (IDB) with a very high density gradient maintains a core region with high density and a temperature of 0.85 keV was achieved when a series of pellets were injected [2]. This operational regime may extrapolate to a high-density and low-temperature ignition scenario for heliotron/stellarator devices.

To study the confinement properties of SDC/IDB plasmas, the accurate reproduction of the MHD equilibrium including the calculations of the bootstrap current is necessary. The local bootstrap current is due to the nature of particle orbits in the presence of local magnetic fields and Coulomb collisions. For nonaxisymmetric toroidal systems, there are several bootstrap current models and approaches. One quasi-analytical fluid moment, the so-called Shaing-Callen approach [3], describes the collisionless asymptote in which the bootstrap coefficient becomes independent of collisionality. This approach is the basis for several numerical tools with self-consistent iterative equilibria: the SPBSC code [4] (NIFS, Japan) and the TERPSICHORE - BOOTSP code [5] (CRPP, Switzerland). These codes can serve to analyze the impact of the bootstrap current on the MHD stability for quite different magnetic configurations in the collisionless (or extreme long-mean-free-

path,  $lmfp$ ) regimes.

Typical LHD experimental discharges and super dense core discharges belong to collisional and highly collisional regimes. For these regimes the Drift Kinetic Equation Solver (DKES) code [6] can perform the bootstrap current calculations, however, for the  $lmfp$  regime this code often provides transport coefficients with large uncertainties depending on the specific magnetic configuration [7].

Recently a new tool, the 3D code VENUS+ $\delta f$ , based on the VENUS numerical orbits, the Monte Carlo technique using the Lorentz collision operator, and the  $\delta f$  weighting scheme for gyrokinetic particle simulation was presented [8]. The VENUS+ $\delta f$  code calculates the diffusion and the bootstrap current coefficients for the general 3D case and for all collisionality regimes without semi-analytical formulas and approximations applied in the SPBSC and TERPSICHORE-BOOTSP codes. For the Wendelstein-7X configuration, the universal VENUS+ $\delta f$  code was able to perform the bootstrap current calculations in the transition region [9] between the extreme  $lmfp$  semi-analytical Shaing-Callen limit and the low collisionality regime, where the DKES code provided the results with large error bars. The extensive benchmarking of the mono-energetic bootstrap current coefficients with the radial electric field for Wendelstein-7X, NCSX and old LHD heliotrons/stellarators configurations was obtained recently [9] by quite different codes — VENUS+ $\delta f$ , DKES, GSRAKE and NEO.

In this paper we present the LHD experimental boot-

author's e-mail: isaev@nfi.kiae.ru

strap current results and the bootstrap current coefficients, calculated with the VENUS+ $\delta f$  code for real LHD vacuum configurations with different magnetic axes, on different magnetic surfaces and in different collisionality regimes. These coefficients provide us the base for the accurate calculations of the total bootstrap current in the LHD experiments in the near future.

The paper is organized as follows. Section 2 describes the LHD experimental bootstrap current results for the typical collisional regime, the SPBSC code theoretical predictions and the bootstrap current coefficient results with the VENUS+ $\delta f$  code. Section 3 describes the VENUS+ $\delta f$  results for the super dense (high collisionality) regime. Section 4 shows the benchmark of the bootstrap current coefficient calculations between the known DKES code results and with the VENUS+ $\delta f$  code for one old test LHD model configuration. Section 5 describes the bootstrap current effect on the  $\iota = 1$  islands, calculated with the VENUS+ $\delta f$  code. In Sec. 6, the main results and future plans are discussed.

## 2. The Bootstrap Current in the Typical LHD Collisional Regime

For the bootstrap current in LHD configurations, there are some early papers. From theoretical predictions based on the quasi-analytical fluid moment approach, the dependence of the bootstrap current on the magnetic configurations and collisionalities has been calculated [4, 10]. From experimental measurements of the non-inductive current, the dependence of the bootstrap current on the beta value and the magnetic configurations were studied, and compared with the theoretical expectations [11]. Figure 1 shows the dependence of the total bootstrap (non-inductive) current obtained experimentally for LHD mag-

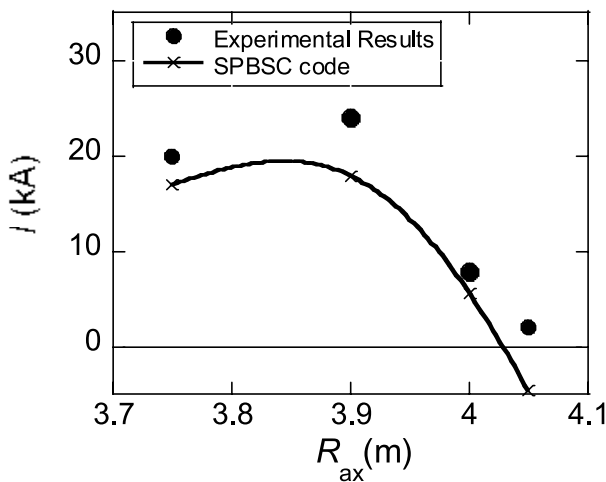


Fig. 1 The magnetic axis position dependence of the experimental bootstrap current and the bootstrap current from the SPBSC predictions.

netic configurations with different magnetic axis locations. In Fig. 1, the electron temperature on the axis  $T_{e0} = 1 \sim 2$  keV and the electron density  $n_{e0} = 1 - 3 \times 10^{19} \text{ m}^{-3}$ . These parameters correspond to the normalized collision frequency  $\nu^* \leq 1$ ; the  $\beta$  values lay in the range 0.33 - 0.41%. Additional experimental setup description and the details are given in [11].

Circles in Fig. 1 denote the experimental data and a line denotes the theoretical predictions of the bootstrap current by the SPBSC code. The experimentally obtained bootstrap currents are from 5 - 8 kA larger than the SPBSC predictions. The maximal positive bootstrap current 25 kA was experimentally obtained for the configuration with the magnetic axis  $R_{ax} = 3.90$  m. An outward shift of the magnetic axis leads to a decreasing of the toroidal current. According to SPBSC predictions, the configuration with the  $R_{ax} = 4.05$  m can have a negative bootstrap current of -5 kA, however, the experimental measurements yield between -2 and +2 kA (depending on the different temperature and density values).

In order to approach the LHD experimental results in this paper, we calculate for the same LHD configurations with the VENUS+ $\delta f$  code the dimensionless bootstrap current coefficient  $D_{31}^*$ , normalized to the collisionless asymptote  $\Delta_0$  [7, 12, 13],

$$\Delta_0 = 0.9733 \sqrt{R/r} / (\iota B_0), \quad (1)$$

of an equivalent large-aspect-ratio tokamak with circular cross section. Energy convolution with the Maxwellian distribution function yields a factor 1.46 instead of 0.9733. The dimensionless bootstrap current coefficient  $D_{31}^*$  is a convenient parameter to compare the sign, the scale and the configuration dependence of the bootstrap current in the different systems.  $D_{31}^*$  depends on the collision frequency, plasma major and minor radii, the radial electric field, and is proportional to the geometric factor of the magnetic configuration [12]. The total bootstrap current will be obtained via the energy convolution and the integration over the flux surface of the local bootstrap current density database for the different plasma surfaces [4, 6].

To calculate the dependence of the LHD bootstrap current coefficients  $D_{31}^*(R_{ax})$  with the VENUS+ $\delta f$  code, we take several LHD plasma boundary spectra with different magnetic axes, obtained using the real LHD coils as the inputs for the 3D MHD equilibrium code VMEC [14] with finite  $\beta = 0.06\%$ . As the next step, the TERPSICHORE [15] mapping to Boozer magnetic coordinates is performed to obtain the accurate representation of values needed in the drift equations. Solving the drift equations for each particle together with the linear Fokker-Planck equation for the particle weight along the VENUS numerical trajectory, we get the steady-state solution for the bootstrap current coefficient after several collision times. The detailed descriptions of the  $\delta f$  methods for the transport coefficients can be found in Refs. [13, 16].

The typical LHD collisionality regime with effective

normalized frequency  $\nu^* \leq 1$  can be reproduced by the VENUS+ $\delta f$  code using the Lorentz pitch angle scattering [17] with inverse mean-free-path values  $\nu/V = 0.003 - 0.01$  [1/m]. The relationships between the temperature, the density, the effective normalized frequency  $\nu^*$  and the inverse mean-free-path values  $\nu/V$  are presented in Fig. 2, where  $\nu^* = X^* f_t / (1 - f_t) \nu/V$ ,  $f_t$  is the fraction of trapped particles,  $X$  coefficient approximately equals to 100 [10]. Zone A corresponds to the typical collisionality regime, described in Fig. 1 of this section, zone B calculations (high collisionality regime,  $\nu^* \gg 1$ ) corresponds to the typical SDC/IDB plasmas, where the electron temperature is almost flat in the core, and the density is peaked.

Bootstrap current coefficients  $D_{31}^*$  as a function of normalized plasma radii  $r/a = 0.2, 0.5, 0.8$  ( $r/a = 1$  corresponds to the plasma boundary) with different magnetic axes positions, calculated with the VENUS+ $\delta f$  code for the collisional regime with the uniform inverse mean free path  $\nu/V = 0.003$  [1/m] are shown in Fig. 3 (a); Fig. 3 (b) shows the same set of results for the uniform inverse mean free path  $\nu/V = 0.010$  [1/m].

The largest positive bootstrap current coefficient, equal to 0.4, is obtained for the LHD configuration with the magnetic axis  $R_{ax} = 3.90$  m and  $\nu/V = 0.003$  [1/m]. For  $\nu/V = 0.010$  [1/m] the largest positive  $D_{31}^*$  is about 4 times smaller. An outward shift of the magnetic axis decreases the value of  $D_{31}^*$ , the configurations with the magnetic axes  $R_{ax} = 4.05$  m and 4.10 m have negative bootstrap current coefficient for all plasma radii. The bootstrap current coefficient for the configuration with the magnetic axis  $R_{ax} = 3.95$  m is positive near the plasma edge and negative in the middle of the plasma column.

Such tendency of the bootstrap current coefficient behavior agrees qualitatively with the LHD experimental

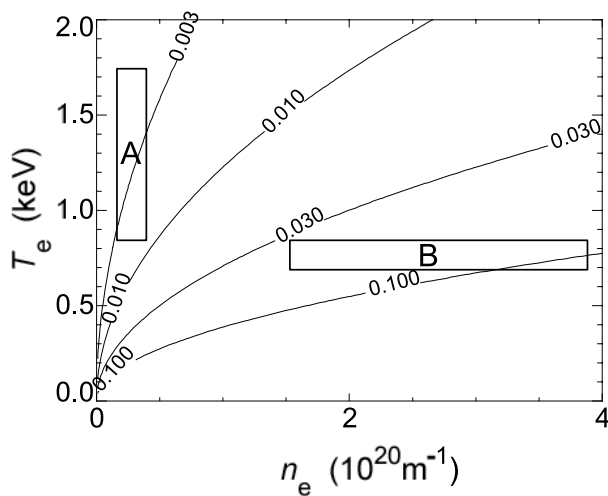


Fig. 2 Typical collisional (zone A,  $\nu^* \sim 1$ ) and high collisional regimes (zone B,  $\nu^* \gg 1$ ) of LHD plasmas in temperature  $T_e$  and density  $n_e$  diagram with the inverse mean free path  $\nu/V = 0.100, 0.030, 0.010, 0.003$  [1/m] contours.

results and with the SPBSC predictions (compare with Fig. 1). In Figs. 3 (a), 3 (b) we do not take into account that in real LHD experiments the collisionality regime is not uniform with respect to the plasma radius. Accurate calculations of the total bootstrap current with the VENUS+ $\delta f$  code using the  $D_{31}^*$  ( $r/a, R_{ax}, \nu/V, E_r$ ) database together with the experimental LHD temperature and density profiles, and the radial electric field  $E_r$ , will be performed in the near future.

SPBSC code results in the case of  $\nu/V = 0.003$  [1/m] shows the same effect that the outward shift has on the normalized geometric factor [4] as we have obtained with the VENUS+ $\delta f$  code for  $D_{31}^*$  (Fig. 4). In the SPBSC code, the bootstrap current in the wide collisional regime is calculated based on a connection formula for the collisionalities [10]. For  $R_{ax} = 3.90$  m this factor is positive for all plasma radii and for the outward shifted configuration with

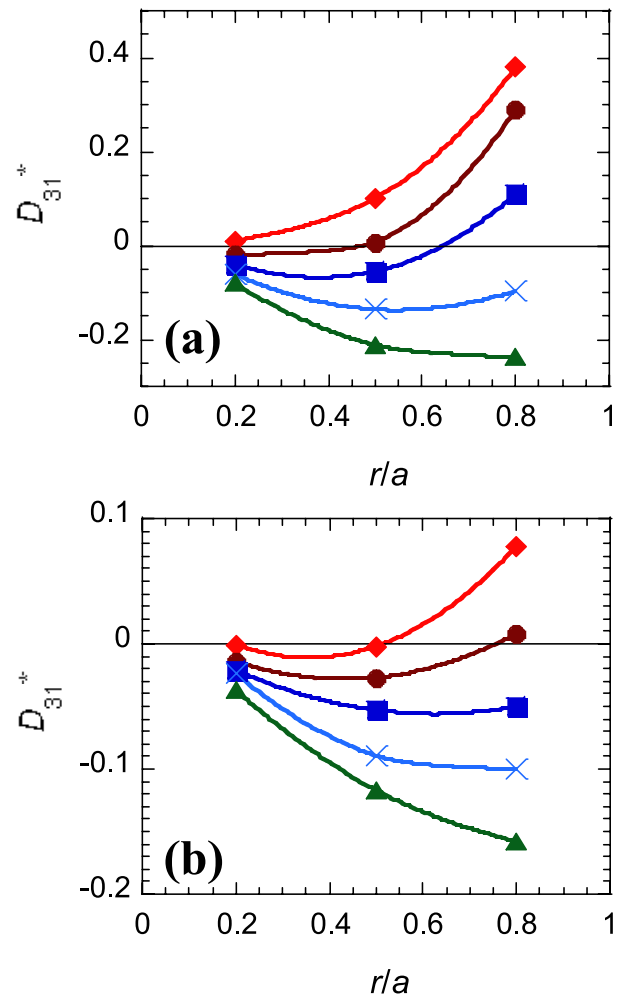


Fig. 3 VENUS+ $\delta f$  bootstrap current coefficients  $D_{31}^*$  versus the normalized plasma radius  $r/a$  for the LHD configurations with different magnetic axes positions  $R_{ax} = 3.90$  m (diamonds), 3.95 m (circles), 4.00 m (squares), 4.05 m (crosses), 4.1 m (triangles) for the collisional regime with  $\nu/V = 0.003$  [1/m] (a) and  $\nu/V = 0.010$  [1/m] (b).

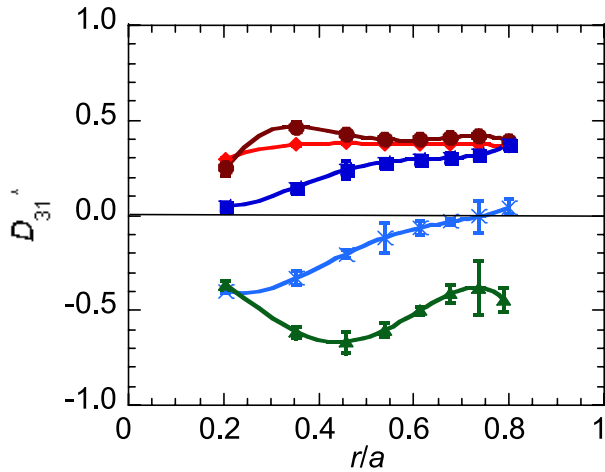


Fig. 4 SPBSC bootstrap current coefficients  $D_{31}^*$  versus the normalized plasmas radius  $r/a$  for the LHD configurations with different magnetic axes positions  $R_{ax} = 3.90$  m (diamonds),  $3.95$  m (circles),  $4.00$  m (squares),  $4.05$  m (crosses),  $4.10$  m (triangles) for the collisional regime with  $\nu_{th}/V_{th} = 0.003$  [1/m].

$R_{ax} = 4.10$  m the geometric factor is always negative. In these SPBSC calculations we used the same temperature profiles for both electrons and ions, so the radial electric field effects on the bootstrap current were eliminated [11].

### 3. The Bootstrap Current in the High Collisionality LHD Super Dense Core Plasma

The LHD SDC/IDB plasma has a set of specific properties [2, 18], and was observed in the LID (Local Island Divertor) configurations. The internal diffusion barrier with a very high-density gradient maintains a core region with high density. A self-consistent free-boundary 3D equilibrium solution with such a large density gradient and externally imposed large island ( $m/n = 1/1$ ) extending over 15% of the minor radius with large Shafranov shift has not yet been found with the existing numerical tools. The plasma configuration has a large Shafranov shift and the magnetic axis is located at the point  $R_{ax} = 4.05$  m.

The VENUS+ $\delta f$  bootstrap current calculations, which assume nested magnetic surfaces as input, cannot exactly reproduce these experimental data. However, in order to approximate the problem, we can consider fixed boundary finite  $\beta$  equilibrium inputs with nested magnetic surfaces, corresponding to the super dense core vacuum plasma boundaries for the high collisionality regime with a uniform inverse mean free path  $\nu/V = 0.03 - 0.1$  [1/m]; see zone B in Fig. 2.

Bootstrap current coefficients  $D_{31}^*$  as a function of normalized plasma radii  $r/a = 0.2, 0.5, 0.8$  ( $r/a = 1$  corresponds to the plasma boundary) for the different magnetic axes, calculated with the VENUS+ $\delta f$  code for the high

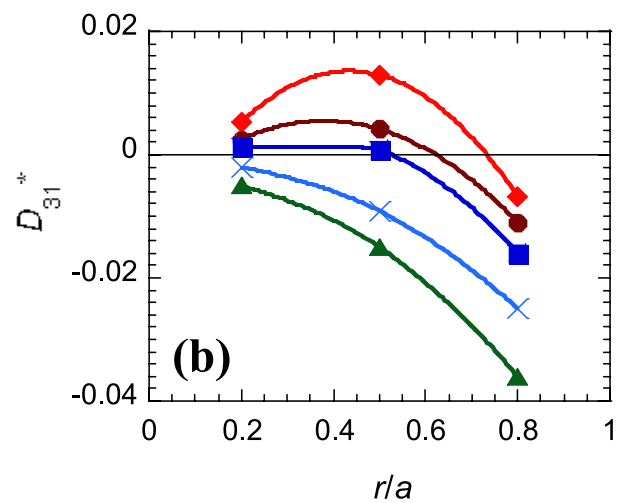
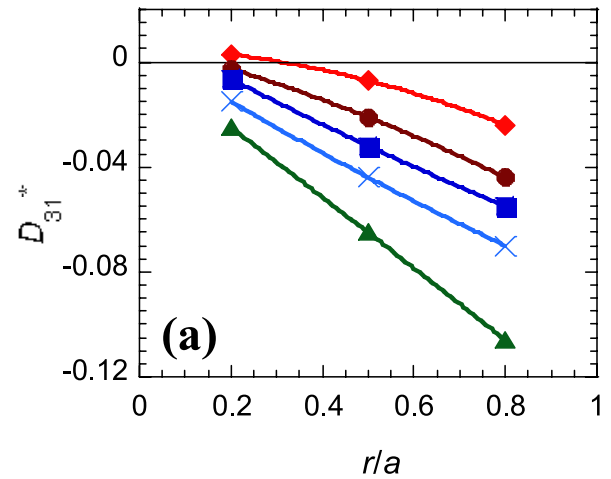


Fig. 5 VENUS+ $\delta f$  bootstrap current coefficients  $D_{31}^*$  versus the normalized plasmas radius  $r/a$  for the LHD configurations with different magnetic axes positions  $R_{ax} = 3.90$  m (diamonds),  $3.95$  m (circles),  $4.00$  m (squares),  $4.05$  m (crosses),  $4.10$  m (triangles) for the high collisional regime with  $\nu/V = 0.03$  [1/m] (a) and with  $\nu/V = 0.10$  [1/m] (b).

collisionality (super dense) regime with uniform inverse mean free path  $\nu/V = 0.03$  [1/m] are shown in Fig. 5 (a). The bootstrap current coefficient is negative and almost linear with respect to the plasma radius in the configurations with the magnetic axes  $R_{ax} = 3.95$  m,  $4.00$  m,  $4.05$  m and  $4.10$  m. For the configuration with the magnetic axis  $R_{ax} = 3.95$  m the bootstrap current coefficient is positive only close to the magnetic axis. The largest negative value of  $D_{31}^* = -0.11$  is found near the plasma edge for the configuration with the magnetic axis at  $4.10$  m. Figure 5 (b) shows the same set of results for the uniform inverse mean free path  $\nu/V = 0.10$  [1/m]. The largest negative coefficient  $D_{31}^* = -0.035$  is still observed in the configuration with the magnetic axis at  $4.10$  m, but for this collisionality regime this value is smaller than for  $\nu/V = 0.03$  [1/m].

One can conclude that the bootstrap current coeffi-

cient for the high collisionality regime  $\nu/V = 0.10$  [1/m] is quite small for all LHD configurations and for all plasma radii, so it is not clear yet whether the total bootstrap current for the super dense core discharges will influence the equilibrium and other plasma properties. Accurate calculations of the total bootstrap current for the super dense core LHD plasmas should take into account the experimentally obtained profiles of the collisionality, density and temperature and will be performed in the near future. Additional problems are connected with the island structure of the magnetic surfaces for the LHD super dense core discharges. We plan to include the island effects into the VENUS+ $\delta f$  code in near future.

#### 4. The Collisionality Dependence of the Geometric Factor of Bootstrap Current

As shown in Sec. 2, the dependence of the  $D_{31}^*$  on the magnetic configuration shows qualitatively similar behavior for the VENUS+ $\delta f$  and SPBSC low collisionality results, but quantitative agreement can not be claimed. A partial explanation is that the VENUS+ $\delta f$  results are for mono-energetic simulation particles whereas SPBSC assumes a Maxwellian distribution of the energies. Additionally, Fig. 6 illustrates that the VENUS+ $\delta f$  and DKES results exceed the LHD Shaing-Callen asymptote over a considerable range of collisionalities and then approach this limit from above at very small  $\nu/V$ ; a similar behavior of the  $D_{31}^*$  results was also obtained for W7-X simulations [7]. The SPBSC algorithm, however, assumes a monotonic increase of  $D_{31}^*$  as one moves from high to low collisionality and thus approaches the Shaing-Callen asymptote from below. As a future task, it is necessary

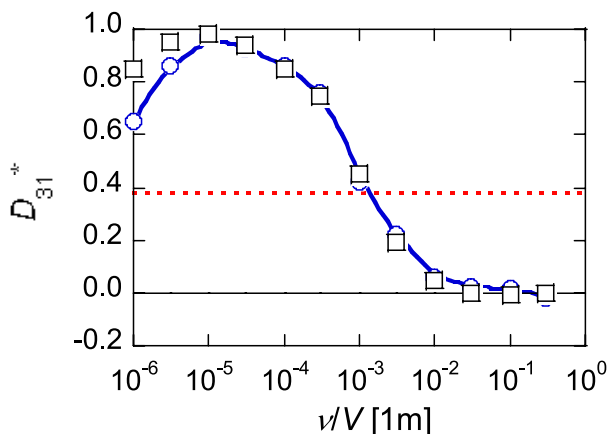


Fig. 6 DKES bootstrap current coefficients (squares), VENUS+ $\delta f$  bootstrap current coefficients (line with circles) and Shaing-Callen limit (dotted line) for the test LHD configuration at  $r/a = 0.5$  with  $R_{ax} = 3.75$  m as a function of the inverse mean free path  $\nu/V$  [1/m] with zero radial electric field.

to investigate the importance of this effect by comparing VENUS+ $\delta f$  results with energy convolution to those of SPBSC result.

The comparison of VENUS+ $\delta f$  and DKES results given in Fig. 6 show excellent agreement except at very low collisionality. In this limit the variational principle employed by DKES indicates increasingly poor convergence of the results; for  $\nu/V = 10^{-6}$  [1/m] the upper and lower bounds on the DKES results differ by  $\pm 10\%$  from their average value which is plotted here. For VENUS+ $\delta f$ , the calculations at these collisionalities require significant computer resources. For example, the VENUS+ $\delta f$  code uses 24 Woodcrest 2.66 GHz processors on the Pleiades2.epfl.ch cluster during 188 hours to get a steady-state bootstrap current coefficient with  $10000 \times 24$  particles and  $1.5 \times 10^7$  time steps for the inverse mean free path  $\nu/V = 3 \times 10^{-6}$  [1/m].

The effect of the radial electric field on the bootstrap current coefficient has been benchmarked using DKES and the VENUS+ $\delta f$  with results for W7-X shown in Ref. [9]. The agreement between the two codes is again good for these comparisons except for similar discrepancies found at the lowest collisionalities investigate.

#### 5. Bootstrap Current Effect on Magnetic Islands

The bootstrap current density plays an important role in the magnetic islands dynamics, including the possible self-healing of the islands width in nearly current-free helical plasmas such as in LHD. According to theoretical predictions (see, for example, [19]), a positive bootstrap current density suppresses the island width when the shear is positive ( $\iota' > 0$ ), a negative bootstrap current density will increase the island size provided the same positive sign of the shear.

Such bootstrap current effects on the magnetic islands have been calculated with the VENUS+ $\delta f$  code for the unperturbed VMEC equilibria with nested magnetic surfaces that have low  $\beta$  and positive shear near the magnetic surfaces with the rational values of the rotational transform  $\iota = 1$ . As follows from Eq. (1), the sign of the bootstrap current coefficient  $D_{31}^*$  corresponds to the sign of the bootstrap current density due to a negative pressure gradient  $dp/dr$ , provided a constant ions and electrons temperature profile. So with these strong restrictions a positive sign of the  $D_{31}^*$  coefficient near the surfaces with  $\iota = 1$  will decrease the island size; a negative sign of the  $D_{31}^*$  coefficient will increase the islands size.

Figure 7 predicts the island dynamics from the  $D_{31}^*$  calculations performed with the VENUS+ $\delta f$  code near magnetic surfaces with  $\iota = 1$  for the LHD configurations with different magnetic axes positions. The configurations with different inward shifted magnetic axes positions  $R_{ax} = 3.50$  m,  $3.55$  m have negative  $D_{31}^*$  coefficient, for all regimes in the range  $\nu/V = 0.003 - 0.1$  [1/m], consequently

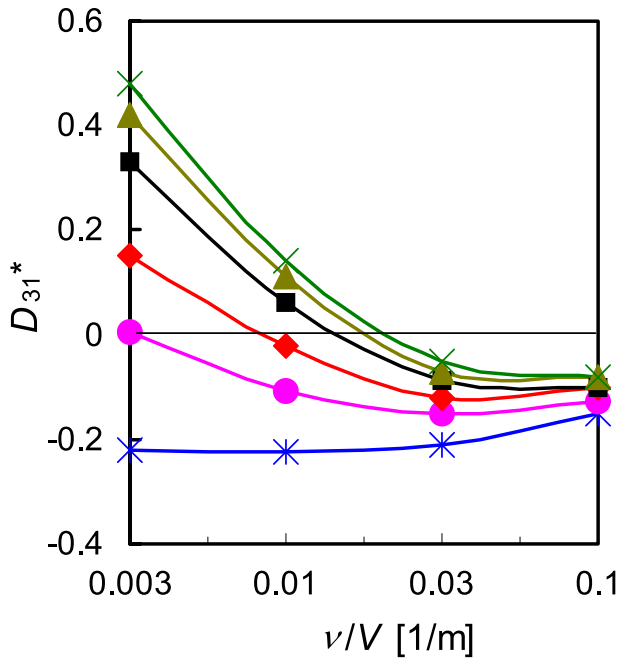


Fig. 7 VENUS+ $\delta f$  bootstrap current coefficients  $D_{31}^*$  as a function of the inverse mean free path  $\nu/V$  near the rational surfaces  $S_i$  with  $\iota = 1.0$  for the LHD configurations with  $R_{ax} = 3.50$  m (stars,  $S_i = 0.83$ ),  $R_{ax} = 3.55$  m (circles,  $S_i = 0.80$ ),  $R_{ax} = 3.60$  m (diamonds,  $S_i = 0.75$ ),  $R_{ax} = 3.65$  m (squares,  $S_i = 0.76$ ),  $R_{ax} = 3.70$  m (triangles,  $S_i = 0.81$ ),  $R_{ax} = 3.75$  m (solid line,  $S_i = 0.83$ ).

the island width will be increased.

For the configurations with the magnetic axes positions  $R_{ax} = 3.55$  m, 3.60 m, 3.65 m, 3.70 m and 3.75 m, the bootstrap current coefficient  $D_{31}^*$  changes sign depending on the collisionality regime. For a high collisionality of the plasma with  $\nu/V = 0.03 - 0.1$  [1/m], the bootstrap current coefficient is negative (the island width will be increased) for cases with  $R_{ax} = 3.60$  m, 3.65 m, 3.70 m and 3.75 m. For collisionless regimes with  $\nu/V = 0.003 - 0.01$  [1/m], these configurations have positive  $D_{31}^*$ , so the island width will be decreased.

These bootstrap current coefficients calculations provide the base for the future bootstrap current density predictions with the experimental temperature and density profiles. Combination of these different profiles can give either negative or positive sign of the bootstrap current [4]. Since the beta effect on the island width as well as the radial electric field effects also should be taken into account, a detailed comparison between the bootstrap current calculations and the LHD experimental data for the different magnetic axes positions, different collisionality regimes and different values of beta will be undertaken in the near future.

Figure 8 shows the  $D_{31}^* = 0$  line as a function of the inverse mean free path  $\nu/V$  and the LHD magnetic axis  $R_{ax}$  near the rational surfaces where the rotational transform,

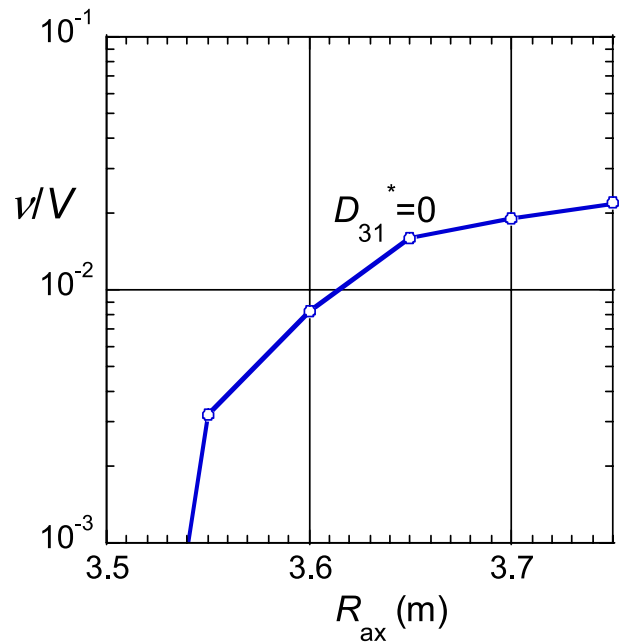


Fig. 8 VENUS+ $\delta f$  bootstrap current coefficients  $D_{31}^* = 0$  contour as a function of the inverse mean free path  $\nu/V$  and the magnetic axis position  $R_{ax}$  near the rational surfaces  $S_i$  with  $\iota = 1.0$  for the LHD configuration.

equals to 1.0. The zone below this line corresponds to positive bootstrap current density (the island width will be decreased), the zone of parameters above the line  $D_{31}^* = 0$  corresponds to a negative bootstrap current density (the island will be enlarged).

## 6. Main Results and Future Plans

This paper describes the bootstrap current coefficient calculations performed with the VENUS+ $\delta f$  code for LHD configurations in different collisionality regimes. Good qualitative agreement of the VENUS+ $\delta f$  code results with the LHD experimental results and with the SPBSC predictions has been obtained provided significant simplifying assumptions for the collisional regime with the inverse mean free paths  $\nu/V = 0.003 - 0.010$  [1/m], which are typical for LHD discharges. The main experimental dependence of the bootstrap current with respect to the magnetic axis outward shift has been reproduced both with the SPBSC and VENUS+ $\delta f$  codes. In accordance with the VENUS+ $\delta f$  calculation in the wide collisionality range, the SPBSC code predictions (semi-analytical Shaing-Callen limit) correspond to the VENUS+ $\delta f$  results for the extreme long-mean-free-path regime ( $\nu/V \ll 10^{-6}$  [1/m]).

On the connection between the semi-analytical Shaing-Callen limit, the SPBSC code predictions, the DKES and the VENUS+ $\delta f$  results for the extreme long-mean-free-path regime remains plagued with numerical difficulties. The DKES code displays there large error bars

for the bootstrap current coefficient. The VENUS+ $\delta f$  code consumes large computer resources to achieve a steady-state solution with small fluctuations. Large fluctuations of the solution are connected with the Monte Carlo method and with a large number of lost particles in the LHD configurations [20]. Possible solutions for the VENUS+ $\delta f$  code are further improvement of the code performance, the usage of new large scalar clusters or vectorisation of the code for corresponding supercomputers [21].

For high collisional regime, the negative bootstrap current is also predicted in the torus-outward shifted magnetic axis configuration. The magnetic axis location, of which bootstrap current is negative, moves more torus-outwardly. However, the IDB/SCD plasma, with  $\nu/V = 0.03 - 0.10$  [1/m], which is the typical high collisionality plasmas in LHD, poses additional difficulties for the bootstrap current calculations connected with the complicated island structure of the magnetic surfaces. The bootstrap current coefficient, calculated for this regime with nested magnetic surfaces by VENUS+ $\delta f$  is relatively small. This result confirms the DKES code calculations, performed for the LHD model configuration. However, accurate calculations of the total bootstrap current for such configurations with an island structure and with real experimental collisionality profiles constitute a future programmatic task. This task is considered as part of a more general problem, meaningful both for tokamaks and stellarators — the problem of transport calculations in real 3D configurations with self-consistent island equilibria [22].

On the bootstrap current effects on the island in  $\iota = 1$  surface, the direction of bootstrap current is sensitive to the magnetic configurations and the collisionality. In more torus-outward shifted magnetic axis configuration with more collisionless plasmas, the healing effect due to bootstrap current is expected more effective.

## Acknowledgements

The authors thank S.P. Hirshman for providing us the VMEC code. The work was supported by NIFS/NINS under the Project of Formation of International Network

of Scientific Collaborations (Japan), by NIFS under Contract No. NIFS06ULHH519, by the Fond National Suisse pour la Recherche Scientifique, by Max-Planck Institute für Plasmaphysik, by Euratom, by the Department of Atomic Science and Technology, RosAtom (Russia).

The computational results were performed at the Pleiades2 cluster (EPFL, Switzerland), on the NEC-SX8 and Opteron cluster (NIFS, Japan), and at the RZG (Garching, Germany).

- [1] O. Motojima *et al.*, Nucl. Fusion **43**, 1674 (2003).
- [2] N. Ohyaabu *et al.*, Plasma Phys. Contr. Fusion **48**, B383 (2006).
- [3] K. Shaing and J. Callen, Phys. Fluids **26**, 3315 (1983).
- [4] K.Y. Watanabe *et al.*, Nucl. Fusion **32**, 1499 (1992).
- [5] W.A. Cooper *et al.*, Plasma Phys. Control Fusion **44**, B357 (2002).
- [6] W.I. Van Rij and S. Hirshman, Phys. Fluids B **1**, 563 (1989).
- [7] C.D. Beidler *et al.*, Proc. 14th Int. Stellarator Workshop, Greifswald, Germany 2003.
- [8] M.Yu. Isaev *et al.*, Fusion Sci. Technol. **50**, 440 (2006).
- [9] K. Allmaier *et al.*, CDROM with Proc. Of Joint Conf. of 17th Int. Toki Conf. on Physics of Flow and Turbulence in Plasmas and 16th Int. Stellarators/Heliotrons Workshop, 2007, P2-029. P.615.
- [10] K.Y. Watanabe *et al.*, Nucl. Fusion **35**, 335 (1995).
- [11] K.Y. Watanabe *et al.*, J. Plasma Fusion Res. SERIES **5**, 124 (2002).
- [12] F. Hinton and R. Hazeltine, Rev. Mod. Phys. **48**, 239 (1976).
- [13] A. Boozer and H. Gardner, Phys. Fluids B **2**, 2408 (1990).
- [14] S. Hirshman and J. Whitson, Phys. Fluids **26**, 3553 (1983).
- [15] D. Anderson *et al.*, J. Supercomput. Appl. **4**, 34 (1990).
- [16] A. Bergmann, A. Peeters and S. Pinches, Phys. Plasmas **8**, 5192 (2001).
- [17] A. Boozer and G. Kuo-Petravich, Phys. Fluids **24**, 851 (1981).
- [18] N. Ohyaabu *et al.*, Phys. Rev. Lett. **97**, 055002 (2006).
- [19] M. Mikhailov and V. Shafranov, Nucl. Fusion **30**, 413 (1990).
- [20] A. Wakasa *et al.*, J. Plasma Fusion Res. SERIES **6**, 203 (2004).
- [21] S. Satake *et al.*, Nucl. Fusion **45**, 1362 (2005).
- [22] E. Poli *et al.*, Plasma Phys. Control Fusion **45**, 71 (2003).